

# *In situ* laser irradiation of WC-Co hardmetals inside an SEM

## Part 1 *General features of surface modification*

H. MUELLER, K. WETZIG, B. SCHULTRICH

*Akademie der Wissenschaften der DDR, Zentralinstitut für Festkörperphysik und Werkstofforschung, Helmholtzstrasse 20, DDR-8027 Dresden, East Germany*

S. M. PIMENOV, N. I. CHAPLIEV, V. I. KONOV, A. M. PROCHOROV

*Institute of General Physics, Academy of Science of the USSR, Vavilova Street 38, 117 333 Moscow, USSR*

Samples of WC-6% Co hardmetals were irradiated with a pulsed CO<sub>2</sub> laser inside a scanning electron microscope in order to study the mechanisms and development of surface modification in microscopic detail. The photon emission of the irradiated surface was measured simultaneously. Samples with surfaces prepared in different ways were irradiated in a multiple pulse regime. The laser power density was somewhat lower than that which would lead to a melting of the polished surface. It is shown that under such irradiation conditions the decisive step in surface modification is the successive solution of the carbide in the lower melting binder phase. Above a critical number of laser pulses, in the order of a thousand, this leads to the onset of large-scale melting, pointing to a marked rise of absorbency. These alterations of surface state are well reflected in the photon emission measurements. The influence of the original binder distribution within the surface layer, changed by grinding or polishing, is investigated.

### 1. Introduction

For hardmetals both an increased hardness and wear resistance can be observed after laser irradiation [1-6]. However, such improved properties are often spoiled by thermal cracking, increased surface roughness and other damage [7]. Similar effects are also observed after electron irradiation [8]. A deeper understanding of these processes and of the high-temperature interaction between the components of the composite material gives the chance to avoid these disadvantages.

Most of the investigations mentioned above did not consider the underlying processes apart from unproved statements that the increase in hardness could be caused by the formation of other carbide phases (W<sub>2</sub>C or metastable cubic β-WC<sub>z</sub>), grain refinement or by binder strengthening. In experiments with electron irradiation, the partial dissolution of the carbide skeleton and the resulting formation of a dendritic solidification structure in the binder were shown [8]. A crude picture of melting, dissolution and precipitation processes was derived by some of the authors from structural alterations after irradiation with a neodymium-glass laser [6, 7]. In this report these mechanisms are investigated in more detail using controlled surface modification by laser multi-pulse irradiation and the capabilities of *in-situ* observations and measurements inside a scanning electron microscope (SEM).

As well as their great practical importance as tool

materials, WC-Co cemented carbides represent an interesting model system for composite consisting of two complementary components as a hard and brittle refractory phase (WC) and a ductile metallic binder (cobalt with dissolved tungsten and carbon). In such a combination of a high and a lower melting component (Co(W, C) at about 1350°C [9] and WC at about 2700°C) unambiguous temperature marks are made. These different melting points, in combination with the different optical absorbencies of WC and Co, may cause special interaction effects between the hard material WC and the cobalt binder phase. The *in situ* surface modification by laser irradiation inside an SEM is a powerful method of studying these processes in microscopic detail.

The present paper of this work (Part 1) deals with the general features of surface modification during multi-pulse laser irradiation of WC-6% Co hardmetals with different initial surface states. In the following part, Part 2, which will be published later, the cobalt binder will be discussed in more detail [10].

### 2. Experimental conditions

The hardmetals investigated contain WC grains as dominating phase (mean crystal size 1 to 2 μm) and 6 wt % Co (corresponding to 10 vol %). These compact composite materials consist of a connected skeleton of carbide grains where the remaining space is filled with binder material. The samples were applied with different surface states: as received

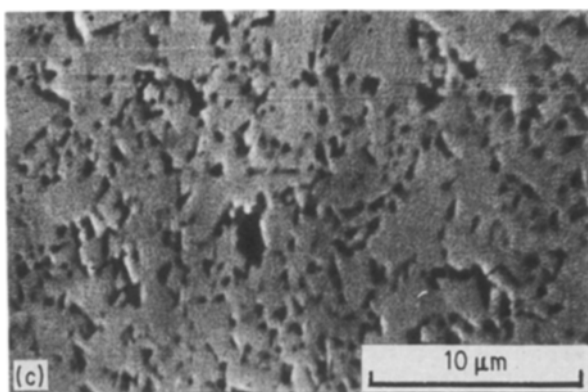
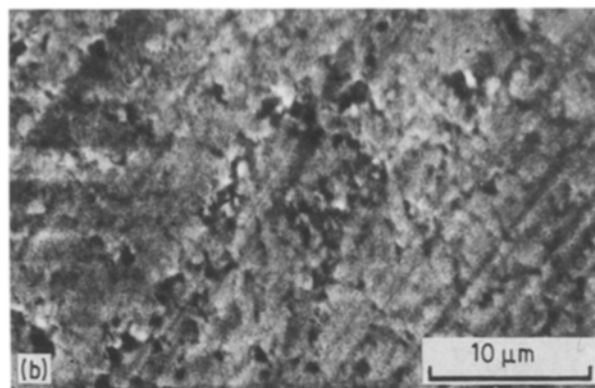
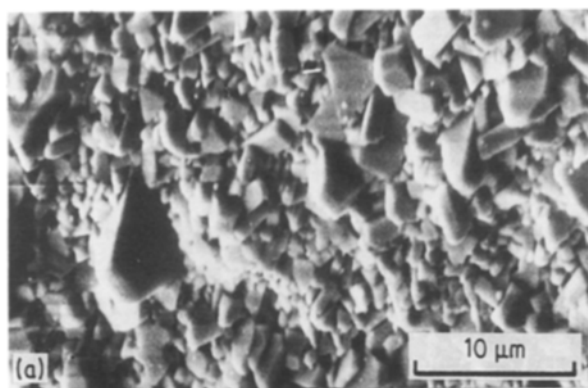


Figure 1 Different surface states of WC-6% Co hardmetals: (a) as-received, (b) ground, (c) polished.

from sintering, ground or mechanically polished. In addition to roughness (mean value 1, 0.3 and 0.1  $\mu\text{m}$ , respectively), they differ in composition of surface region, in defect structure and in internal stresses. After sintering, the samples show well-crystallized carbide grains on their surfaces (Fig. 1a), leading to a roughness of the order of the grain size. The binder is evaporated from this region during sintering. This process gives rise to open pores and deep holes. By grinding with diamond wheels this surface region, deviating from the interior, is removed and the roughness is reduced. However, the grinding action of the diamond grains causes strong plastic deformation and partial fracture of the superficial carbide crystals (Fig. 1b). Furthermore, a thin cobalt film is smeared

over the structural details. Compressive stresses of the order of 1 GPa are induced up to a depth of 30  $\mu\text{m}$  [11]. By polishing, the distorted grinding layer is removed. The surface structure of polished samples corresponds to a geometrical cross-section through the material (Fig. 1c). In an SEM image, the bright polygonal grains correspond to the hexagonal WC crystals and the dark region between them to the binder phase. Careful polishing eliminates almost all of the plastically induced grinding stresses and structural defects. The latter fact is of importance in the optical behaviour. For the related titanium carbide, it was proved that reflectivity increased with decreasing size of polishing grains due to the smaller distortion and that it approximates the reflectivity of perfectly grown single crystals [12]. The reflection coefficient of a polished WC-6% Co sample was measured in dependence on wavelength (Fig. 2). In accordance with laser irradiation conditions, an angle of incidence of 45° was selected. At 10  $\mu\text{m}$  wavelength, a reflection of 88% was found in comparison to a gold standard with a reflection coefficient of nearly 100%, i.e., for the polished samples, about 12% of the incident energy is absorbed. For the other surface states a higher absorbed fraction can be assumed as supported by direct absorption measurements on these materials at 1  $\mu\text{m}$  wavelength [13].

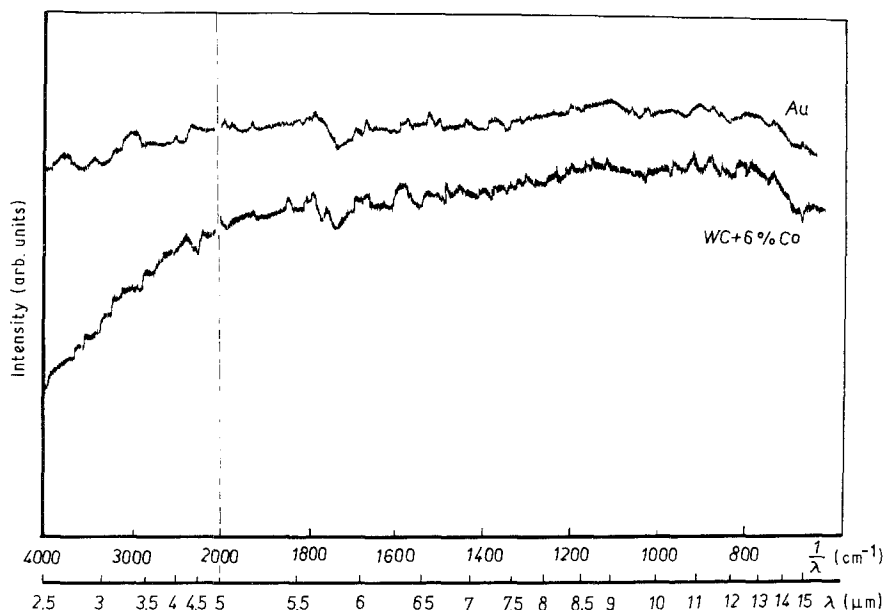


Figure 2 Dependence of reflectivity of a polished WC-6% Co hardmetal on wavelength (angle of incidence 45°).

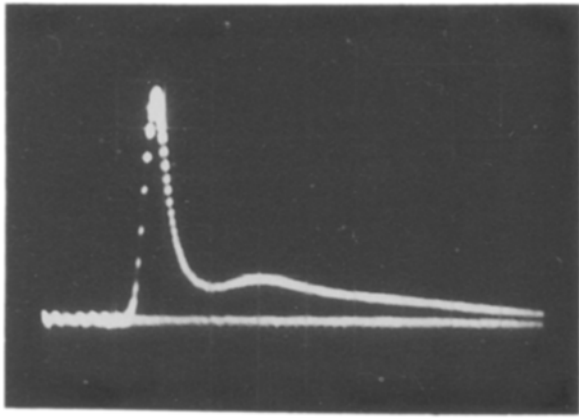


Figure 3 The shape of the laser pulses.

The samples ( $5 \times 5 \times 20 \text{ mm}^3$  in size) were irradiated inside a scanning electron microscope (model MREM-100) with a  $\text{CO}_2$  laser (model 143 [14]) at an angle of incidence of  $45^\circ$ . The pressure inside the sample chamber was about  $1.3 \times 10^{-4} \text{ Pa}$  produced by a magnetic discharge pump. The laser was operating in the ground mode of energy distribution ( $\text{TEM}_{00q}$ -mode) with a maximum energy output of about 50 mJ. It was possible to attenuate the incident energy with the aid of calibrated  $\text{CaF}_2$  filters. The temporal shape of the laser pulse is shown in Fig. 3. Within the sharp spike of 100 nsec half-width, 50% of the whole laser pulse energy is concentrated. The total pulse duration is about  $2.5 \mu\text{sec}$ . In order to measure the energy distribution within the laser beam, a developed photographic film placed in the focal plane was irradiated with different energies,  $E$ . Then the diameters,  $d^* = 2r^*$ , of the molten gelatinous area corresponding to a characteristic energy density,  $q^*$ , were measured. From the relation  $q^* = f(r^*)E$ , the

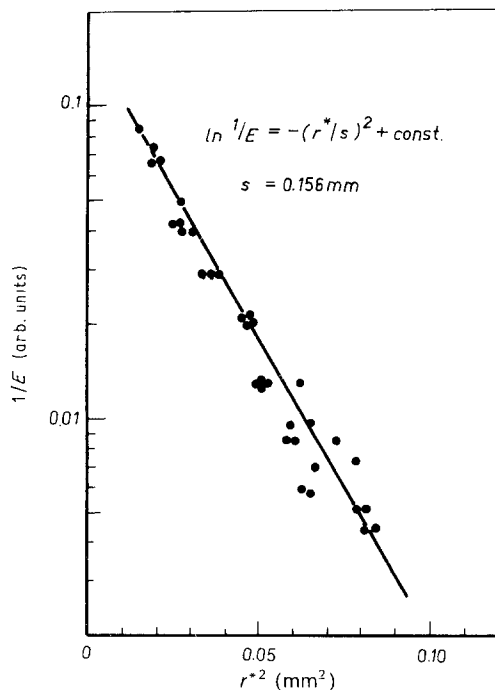


Figure 4 Logarithm of energy plotted against square of the characteristic radii, representing the lateral energy distribution of the laser beam.

reciprocal of the incident energy,  $E$ , in dependence on the corresponding radii,  $r^*$ , yields directly the energy distribution function,  $f(r)$ . Plotting  $\ln(1/E)$  or  $\ln(E)$  against  $r^{*2}$  gives a straight line (Fig. 4), proving the Gaussian beam profile  $q(r) = q_m \exp(-(r/s)^2)$ . For the characteristic decay length,  $s$ , with  $q(s)/q_m = 1/e = 0.37$  it follows  $s = 0.156 \text{ mm}$ . A comparison with the total energy  $E = 2\pi \int q(r)r dr = \pi s^2 q_m$  yields the maximum energy density,  $q_m$ , in the spot centre. For the energy  $E = 24.2 \text{ mJ}$ , used for the irradiation experiments discussed below, we obtain  $q_m = 31.6 \text{ J cm}^{-2}$  and corresponding peak power densities of about  $160 \text{ MW cm}^{-2}$ .

During laser irradiation inside the SEM, the photon emission of the sample was measured simultaneously with the aid of a photomultiplier (PHM). The arrangement was adjusted carefully to exclude any influence of reflected laser light or luminescence of the chamber wall on the PHM. In this way the *in situ* investigation of the laser effects by electron microscopy is combined with simultaneous observation of the process by means of its photon emission (PE).

### 3. Results of photon emission measurements

The photon emission of the surface irradiated by laser pulses gives a rough measure of the response of the material to irradiation. Its intensity indicates the degree of interaction between radiation and material and therefore should be related to the quality of the surface after irradiation. The special nature of this change can only be revealed by more detailed methods, especially electron microscopic observation (see Section 4). Nevertheless, due to its averaging and, at the same time, quantitative nature, the photon emission intensity is well-suited for an initial characterization of the complex phenomenon.

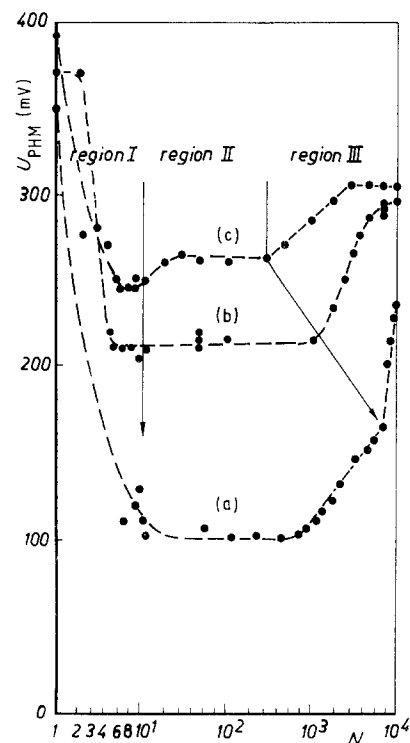


Figure 5 Luminescence intensity plotted against the number of laser pulses: (a) polished, (b) ground, (c) as-received surfaces.

The sample responds to the first pulse by intense photon emission (Fig. 5) which decreases drastically during the following pulses (region I). The intensity of the initial emission is nearly equal for all samples (about  $370 \pm 20$  mV on the PHM), i.e. independent of initial surface roughness. After about ten pulses a minimum is reached. During the next several hundred pulses the intensity remains at a nearly constant level (region II). It lies at a higher level for the samples with larger surface roughness. Suddenly, however, the photon emission increases rapidly, indicating larger structural changes and damage on the surface (region III). The onset of this process depends on the surface quality at the beginning of laser irradiation (Fig. 5) and on the incident power density. With a constant peak power density of  $160 \text{ MW cm}^{-2}$  this catastrophic damage occurs after about 300 pulses for the surface as-received from sintering, and after about 1000 pulses for the ground surface. The polished sample shows a more complex behaviour with the first changes at about 1000 pulses and a steeper rise of PE intensity above 6000 pulses. For larger pulse numbers the photon emission seems to saturate at a level nearly independent of the initial surface state.

#### 4. Electron microscopical investigation

The special arrangement for laser irradiation within the SEM allows direct observation of the gradual development of the surface structure at high magnifications.

The polished surface shows the following behaviour. After the first few laser pulses (region I, Fig. 5) changes are hardly detectable. Some relief contrast, characterized by bright edges, starts to develop at the binder-carbide interfaces. This becomes successively more distinct up to about 500 pulses (Fig. 6a). The original grains and their arrangement remain stable but instead of the sharp rectilinear phase boundaries, rounded drop-like structures occur, overlapping the carbide grains. This suggests that due to the excellent wetting of WC by liquid cobalt [15] the binder starts to creep over the carbide surface, wrapping the smaller grains and building fine binder walls on the larger ones. At about 1000 pulses they are all covered by a thin binder film, temporarily molten as revealed by traces of small inhomogeneities on the carbide surfaces (Fig. 6b). This layer thickens more and more, gradually covering the original surface grains (Figs 6c to e). Careful comparison shows that notwithstanding the melt effects, many structural details remain constant or only change gradually. This phenomenon and the crumbly appearance of the melt surface with many open pores point to little fluidity during the melting stage. Furthermore it must be emphasized that the formation of the molten layer does not proceed by melting at the carbide grains, but by its successive dissolution in the lower melting binder phase. Thermal cracks appear only in later states where the whole surface is covered by a molten layer (Figs 6e, f). Finally, after 6000 or more pulses the surface layer remelts to a nearly structureless appearance, microscopically plane but macroscopically very uneven. Large cracks are formed, which may disappear again or may be overlaid by the melt.

The structural development of the ground samples differs from that of the polished ones at least in its early stages. The first laser pulse changes the surface structure markedly (Fig. 7a): the grinding marks are eliminated and the detailed carbide grain arrangement (previously nearly invisible because of the thin cobalt film covering the sample surface after grinding) appears. The elimination of grinding marks without alteration of the carbide grains shows that at least the smaller ones are only grooved into the covering binder film but not into the hard phase itself. The higher contrast of the grain arrangement is not caused by cleaning the carbide surfaces of their covering, amplifying material, but rather by additional creep of binder material towards the carbide, leading to larger relief contrast. This becomes clearly visible after more laser pulses where the surface successively takes on a more rounded and wavy appearance (Fig. 7b). Notwithstanding these viscous effects, there is no fundamental rearrangement of the surface structure and characteristic details of the original surface can be related to the irradiated one, up to 100 pulses (Fig. 7c). At this stage some new effects appear. In addition to the start of thermal cracking there is the formation of many very fine pores of the order of  $0.2 \mu\text{m}$  in size all over the surface (Fig. 7d). Presumably they are caused by boiling effects in the viscous melt. On the other hand, the larger pores, visible at lower pulse numbers, which are connected to the original binder regions, successively disappear. Above 1000 pulses the surface of the stiffened melt becomes locally even. The original surface is transformed to larger drop-like melt tongues (Fig. 7e). In particular, at higher pulse numbers, the melt contracts under the action of surface tension forming larger drops revealing the carbide grains below the molten layer (Fig. 7f).

With the as-received surface there are no observable changes after the first few pulses (Fig. 8a). After about ten pulses some grains begin to round off (Fig. 8b). This seems to occur preferably at larger grains extending into deeper layers, whereas neighbouring smaller ones remain unaffected. Hence, it may be anticipated that the evident appearance of melt effects is not caused by direct melting of the tungsten carbide but represents molten binder ascending from subsurface regions. This view is supported by the successive expansion of these melt regions overlying the nearly unchanged carbide grains (Figs 8c, d). The form of the melt fronts is relatively stable and can be followed up to 500 pulses and more (Fig. 8e). In the final stage, the usual picture appears, with large melt drops (partially with fine micropores) and revealed deeper layers of the carbide grains between them (Fig. 8f).

#### 5. Discussion

Investigations of the laser-induced damage of metal mirrors showed the existence of a critical value of power density where surface damage occurs during the first laser pulse accompanied by a light flash (single pulse surface damage) [16]. Below this critical value, surface damage is observed after sufficient multi-pulse irradiation. The number of pulses necessary for this damage decreases with increasing power density.

Finally, successive surface alterations turn to catastrophic damage. This behaviour can be explained by a rise of absorbency and a corresponding rise of the energy input: repeated irradiation leads to an accumulation of plastic deformations [17], in its later stages revealed by increasing surface roughness. The plastic processes are accompanied by higher densities of lattice defects which, together with the increased roughness, raise the absorbency.

For the heterogeneous composite material investigated in this paper, some peculiarities caused by the differences between the two phases and their mutual

interaction must be considered. For an estimation of the influence of the different melting points some information on the temperature field is necessary. The repetition rate of the maximum 100 pulses/min guaranteed a cooling of the irradiated surface down to room temperature between the pulses. This was proved by a rough estimation as well as by photon emission measurements. In spite of the repetition rate of 100 pulses/min the ground photon emission level of the sample surface did not increase. In order to estimate the temperature at the surface, a triangular pulse shape in combination with a rectangular one was

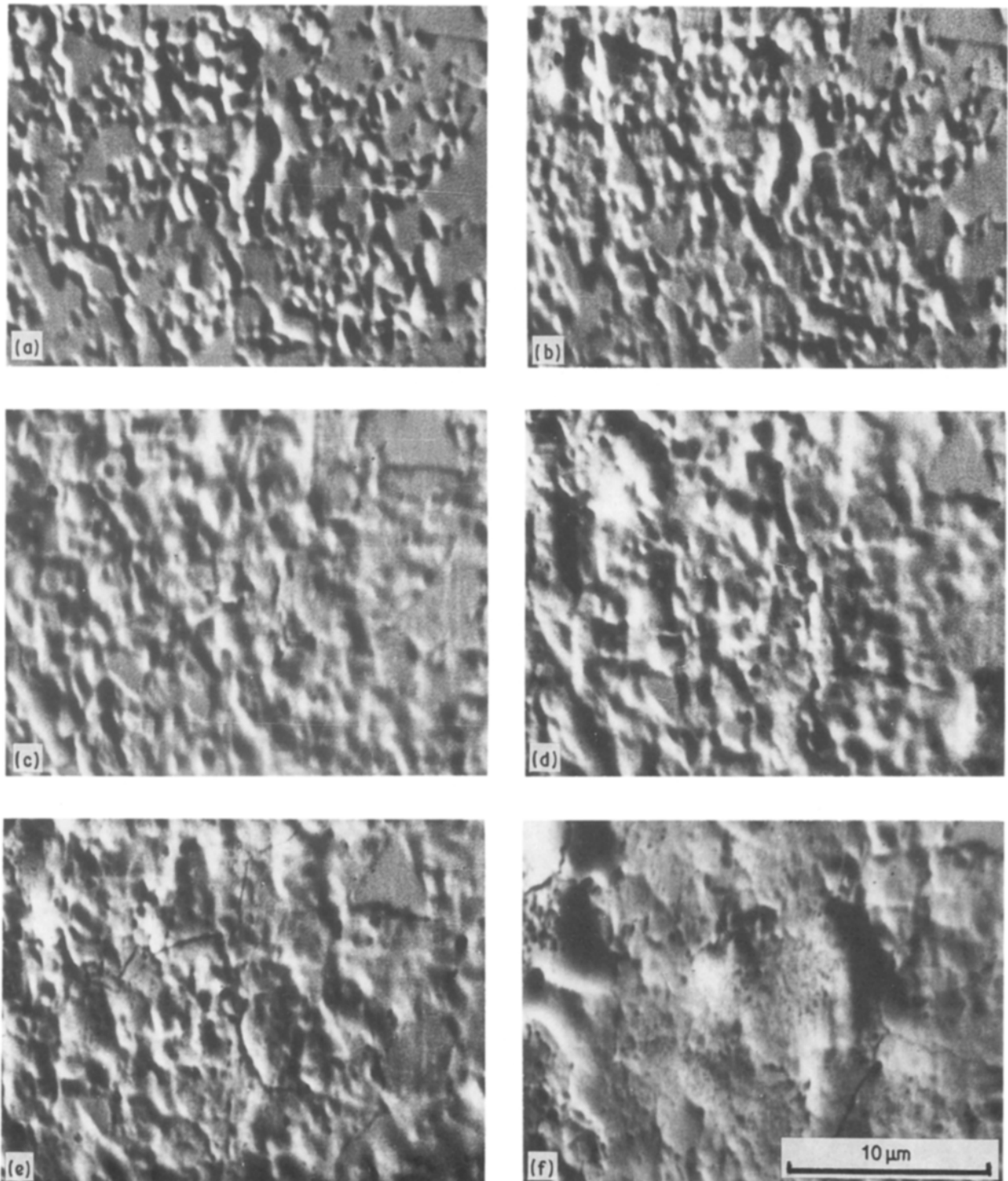


Figure 6 Structural development of a polished WC-6% Co hardmetal on laser irradiation. (a) 500, (b) 1000, (c) 2000, (d) 3000, (e) 4000, (f) 6000 pulses.

assumed, as seen in Fig. 9. This problem can be treated with standard solutions [18]. For the angle of incidence of  $45^\circ$  the maximum energy density alters to

$$q = q_m \cos(45^\circ)$$

As a first approximation, the room temperature values for specific heat,  $c = 210 \text{ J K}^{-1} \text{ kg}^{-1}$ , and thermal diffusivity,  $a = 29 \text{ mm}^2 \text{ sec}^{-1}$ , were used. For polished surfaces, the absorptency,  $\varepsilon = 0.12$ , determined by optical measurements (Section 2) could be taken, neglecting any possible change of absorption behaviour due to the high intensity of laser irradiation. With a power density  $q_1 = 1.21 \text{ J cm}^{-2}$ ,  $q_2 = 1.47 \text{ J cm}^{-2}$  and

durations  $t_1 = 200 \text{ nsec}$  and  $t_2 = 2 \mu\text{sec}$ , this yields for the maximum increase of surface temperature in the spot centre  $\Delta T_m = 2150 \text{ K}$  for the first laser pulse on a polished surface, which lies well above the melting point of the cobalt binder. This seems to be in obvious contradiction to the SEM observations where, at the beginning of multi-pulse laser irradiation, no melting was found at the polished surface. But this high temperature acts only for a very short time of about 200 nsec and in a very thin surface layer of less than about  $1 \mu\text{m}$ . This seems to be insufficient for any remarkable change in surface topology.

For the other two surface states, a higher absorptency

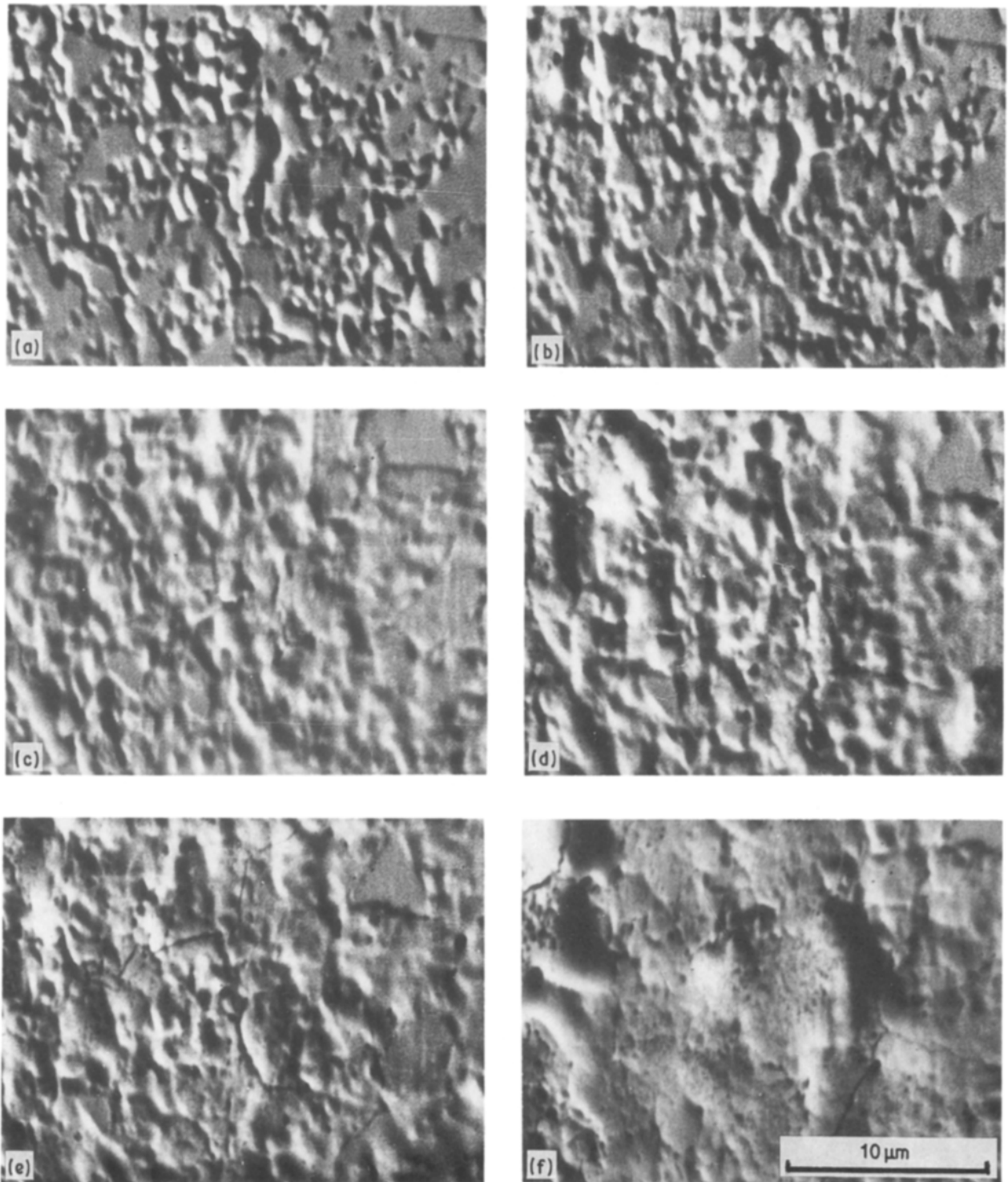


Figure 7 Structural development of a ground WC-6% Co hardmetal on laser irradiation. (a) 1, (b) 2, (c) 50, (d) 100, (e) 2000, (f) 5000 pulses.

must be assumed due to their essential surface roughness and (for ground surfaces) their strong structural perturbation. According to the microscopic observations the maximum temperature already exceeds the melting point of the cobalt binder at the first laser pulse, at least for the ground samples. In this first stage up to about ten pulses (stage I according to Section 3) a uniform behaviour of photon emission characterized by a steep drop from unitary initial value was found. This contrasts with the large differences in the investigated surface states with regard to morphology, composition, perfectness and temperature. Furthermore, no alterations of the surface

structure of the polished or as-received samples were detectable after the first few laser pulses by SEM observation. Hence, it is anticipated that the enhanced photon emission during the first pulses is caused by surface cleaning from contaminations and desorption of gases and is not connected with the modification of the material itself. In the following stage II, the photon emission remains nearly at a fixed level, depending on the initial type of surface: the PE values increase from the polished to the ground and further to the as-received sample. The photon emission should be a measure of the laser energy input and hence likewise correspond with surface temperature.

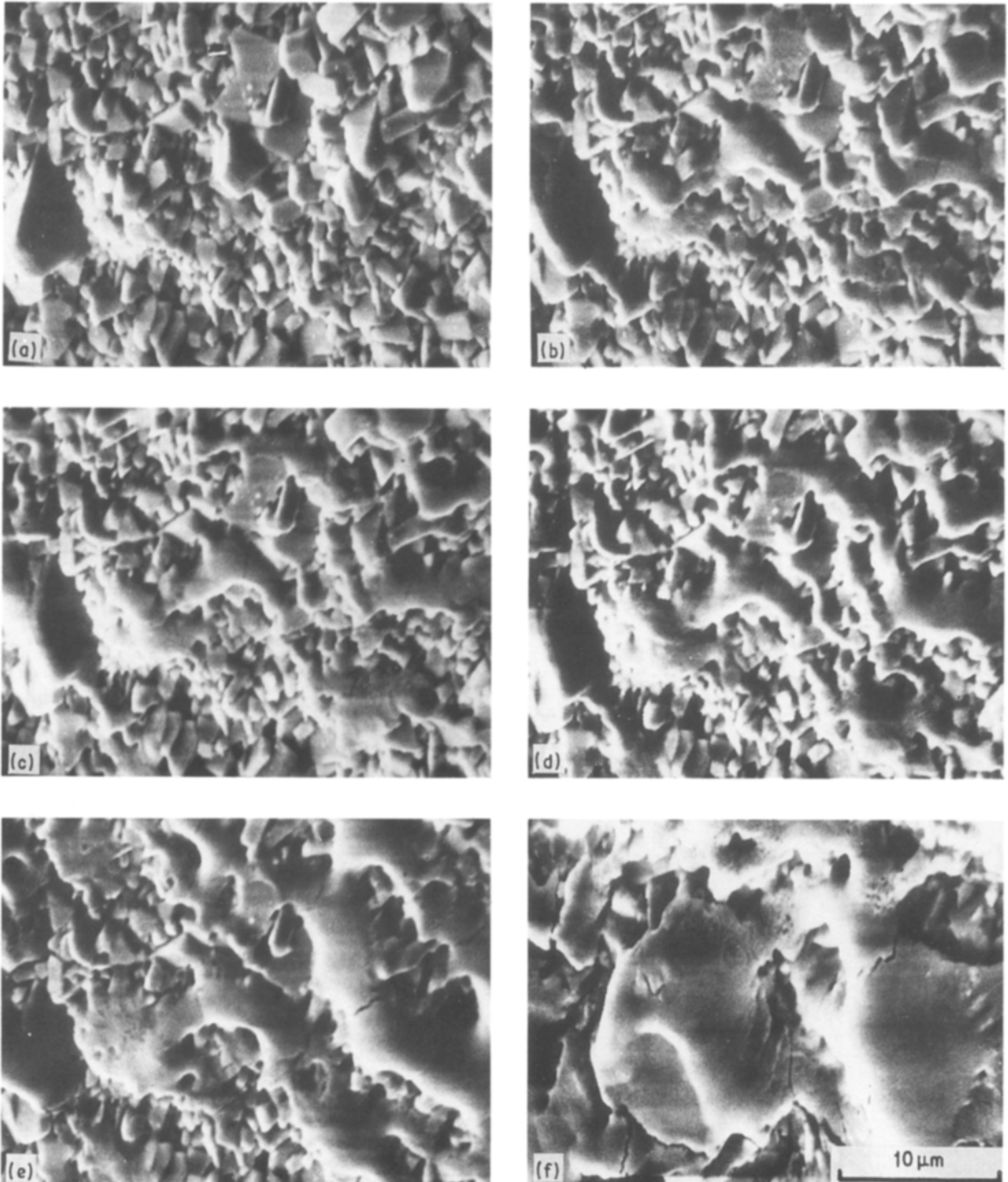


Figure 8 Structural development of as-received WC-6% Co hardmetal on laser irradiation. (a) 1, (b) 10, (c) 50, (d) 100, (e) 500, (f) 2000 pulses.

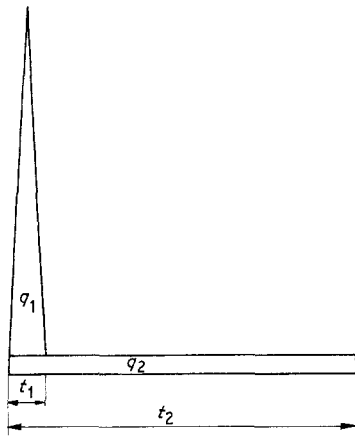


Figure 9 The pulse shape used for numerical calculations.

Indeed the order of the PE values coincides with the expected absorbencies. On the other hand, intense structural transformations occur in the surface layer without equivalent response in photon emission. Hence, it seems that the intensity of photon emission and presumably the absorbency in this stage is more morphologically determined by the roughness of the surface than by its crystalline structure.

For all three types of surface state the laser-induced surface modification is based on the same mechanism: the tungsten carbide is successively dissolved by the molten binder. This process is stimulated by close contact of these two phases and especially by thin cobalt films covering the superficial carbide grains. In the case of ground samples, such a film exists from the beginning as a result of the grinding procedure. Thus the carbide dissolution starts at the first pulse with visible intensity. For the polished and the as-received samples, this covering melt film must be produced first by repeated creep of the binder. Corresponding to their higher roughness, absorbency and surface temperatures this occurs more quickly for the as-received specimens than for the polished ones.

The amount of material incorporated into the melt phase increases with pulse number. This can be attributed to additional binder material ascending

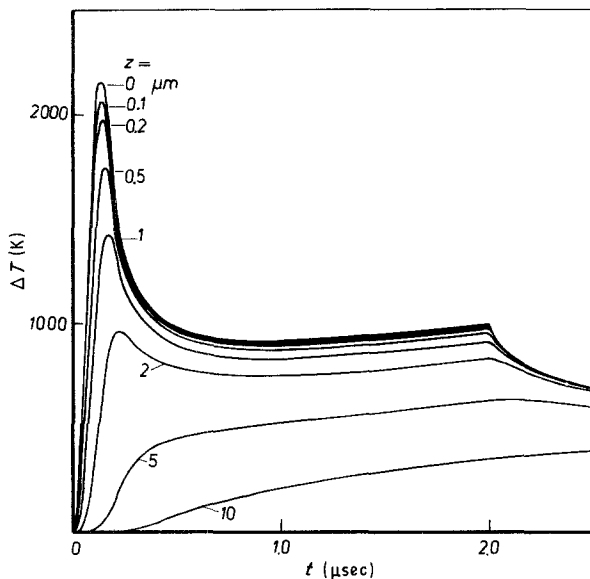


Figure 10 Dependence of temperature at different depths below the surface on time.

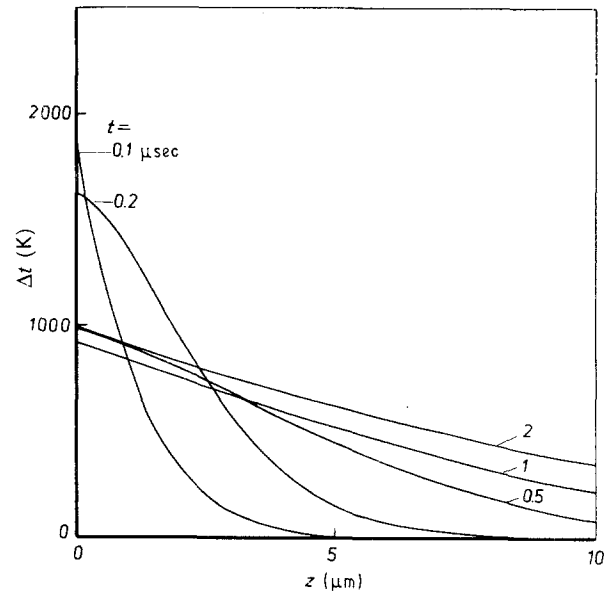


Figure 11 Dependence of temperature at different moments on depth below the surface.

from beneath and to the progressive dissolution of carbide grains, as well. Nevertheless, the surface changes from pulse to pulse are small, often only detectable after many irradiation cycles. At first this high structural stability seems to contradict the observed molten superficial layers. But it may be caused by the existence of an invariable basic structure, which is only overlaid by a thin film of molten binder phase enriched with tungsten and carbide. Furthermore the displacement of the viscous melt is restricted by the duration of the high-temperature stage and by the magnitude of the driving forces. Direction and intensity of the creep processes are controlled by surface tension [10].

The transition to region III of photon emission, characterized by a steep rise in PE intensity, coincides with the formation of large, locally even melt regions, at least in the case of the ground and the as-received samples. This appearance suggests a marked increase in surface temperature near, if not above, the carbide melting point of about 2700°C. For the polished surface the change of PE intensity is more complex: up to about 6000 pulses it corresponds to the approximation towards the surface conditions of the irradiated ground surface in stage II with its much higher level. Only the following steeper ascent seems to be comparable with the II–III transitions for the other surface states, as indicated by the occurrence of similar structural development.

The final region of constant photon emission corresponds to a surface structure which is unchanged by repeated irradiation.

## 6. Conclusions

The structural changes are governed by the interaction of the carbide grains with the lower-melting binder phase. Under the irradiation conditions employed, the carbide is successively dissolved in the lower-melting binder phase. The observed large-scale melting and simultaneous increase in photon emission above a critical number of pulses in the order of thousands,



indicate the onset of a marked rise of absorbency. It was found that the process of surface modification is decisively determined by wetting of WC with cobalt binder and the dissolution of tungsten and carbon in the binder phase. These interaction processes are investigated in more detail in Part 2 of this paper [10].

## References

1. L. I. MIRKIN and N. F. FILIPECKIJ, *Izv. AN SSSR Metall* **3** (1967) 137.
2. E. A. PAMFILOV and T. G. BORZENKOVA, *Vestnik masinostroenija* **3** (1982) 61.
3. E. A. PAMFILOV and T. G. BORZENKOVA, *Masino-stroitel* **11** (1983) 44.
4. E. V. RYŽOV, V. I. AVERČENKOV, V. V. NADUVAEV, O. A. GORLENKO and E. N. FROLOV, *Sverchverdye materialy* **4** (1985) 9.
5. B. SCHULTRICH, H.-J. SCHEIBE, G. KESSLER, M. ERMERICH, H. MUELLER and W. HAUFFE, International Conference on Energy Pulse and Particle Beam Modification of Materials (EPM 87), Dresden (1987) paper 7.9.
6. B. SCHULTRICH, H.-J. SCHEIBE, E. DIESSNER, M. ERMERICH, G. KESSLER and H. MÜELLER, Proceedings Third International Conference "Trends in Quantum Electronics (TQE)", Bucharest (1988).
7. A. H. DARWISH and S. P. ANDERSEN, Quatrieme Symposium Europeen de Metallurgie des Poudres, Grenoble (1975) p. 5.
8. B. ROEBUCK and E. G. BENNETT, *Int. J. Refract. Hard Metals* **6** (1987) 75.
9. G. LEITNER, B. SCHULTRICH, H. KUBSCH, Proceedings of the 7th International Conference on Powder Metallurgy, Vol. I, Pardubice (1987) p. 155.
10. H. MUELLER, K. WETZIG, B. SCHULTRICH, S. M. PIMENOV, N. I. CHAPLIEV, V. I. KONOV and A. M. PROCHOROV, *J. Mater. Sci.* to be published.
11. B. O. JAENSSON, *Mater. Sci. Engng* **8** (1971) 41.
12. K. KOEHLER, Thesis, Universitat Karlsruhe (1981).
13. B. SCHULTRICH, H.-J. SCHEIBE, H. MUELLER, G. KESSLER, M. ERMERICH, to be published.
14. V. V. ATEGHEV, I. N. BARANOV, S. K. VARTAPETOV, V. A. DURKO *et al.*, *Pribory i tehnika eksperimenta* **2** (1983) 248.
15. L. RAMQVIST, *Int. J. Powder Metall.* **1** (1965) A4U 2.
16. CH. LEE, Thesis, University of Southern California (1983).
17. H. M. MUSAL, Jr. in "Laser Induced Damage to Optical Materials", edited by A. A. Glass and A. H. Guenther, NBS Special Publication 568 (National Bureau of Standards, Washington, 1979) p. 159.
18. H. S. CARSHLAW and J. C. JAEGER, "Conduction of heat in Solids" (Oxford University Press, New York, 1959).

*Received 21 March  
and accepted 4 November 1988*